

Combined DØ and CDF Upper Limits on Standard-Model Higgs-Boson Production

DRAFT-INTERNAL WORKING DOCUMENT for CDF and DØ Collaborations ONLY

August 16th

The TEVNPH Working Group*

for the DØ and CDF Collaborations

We combine results of CDF and DØ searches for a Standard-Model Higgs boson (H) in data from $p\bar{p}$ collisions at the Fermilab Tevatron with $\sqrt{s} = 1.96$ TeV. With 1.0-1.9 fb⁻¹ collected at CDF, and 0.9-1.7 fb⁻¹ collected at DØ, the 95% CL upper limits are a factor of 7.8(1.4) higher than the expected cross section for $m_H = 115(160)$ GeV/c². The corresponding expected upper limits are 4.3 (2.5). These results extends significantly the individual limits of each experiment.

I. INTRODUCTION

Because the mechanism for electroweak symmetry breaking has yet to be confirmed, the search for a Standard-Model (SM) Higgs boson is a central part of Fermilab's Tevatron physics program. Both DØ and CDF have recently reported searches for Higgs bosons that combined different final states and production modes[1, 2].

In this note, we combine results of all such searches from CDF and DØ for $p\bar{p}$ collisions at $\sqrt{s} = 1.96$ TeV. These searches are for SM Higgs bosons produced in association with vector bosons ($p\bar{p} \rightarrow W/ZH \rightarrow \ell\nu b\bar{b}/\nu\bar{\nu} b\bar{b}/\ell^+\ell^- b\bar{b}$ or $p\bar{p} \rightarrow WH \rightarrow WW^+W^-$) or singly through gluon-gluon fusion ($p\bar{p} \rightarrow H \rightarrow W^+W^-$). The results are for data corresponding to integrated luminosities ranging from 1.0-1.9 fb⁻¹ at CDF and 0.9-1.7 fb⁻¹ at DØ. The searches are separated into sixteen final states, referred to as analyses in the following. To simplify combination of signals, the analyses are separated into sixteen mutually exclusive final states. Selection procedures for each analysis are detailed in each of the experiment's reports[1, 2], and briefly described below.

II. ACCEPTANCE, BACKGROUNDS, AND LUMINOSITY

Event selections are similar for the corresponding CDF and DØ analyses. For the case of $WH \rightarrow \ell\nu b\bar{b}$, an isolated lepton (electron or muon) and at least two jets are required, with one or more jets tagged as originating from b -quarks. For the DØ $WH \rightarrow \ell\nu b\bar{b}$ analyses, two orthogonal tagging criteria are defined, one being an exclusive single-tag (ST) and the other a double-tag(DT) selection. For the CDF $WH \rightarrow \ell\nu b\bar{b}$ analyses, a selection with two tight b-tags (TDT) is combined with one with one tight b-tag and one loose b-tag (LDT). Selected events must also display a significant imbalance of momentum in the plane transverse to the beam axis (referred to as missing energy or \cancel{E}_T). Events with additional isolated leptons are vetoed. In the $WH \rightarrow \ell\nu b\bar{b}$ analyses, both CDF and DØ use neural network discriminant variables as the final variables used to set limits. These networks are optimized at each value of the Higgs boson mass under study (the "test mass").

For the $ZH \rightarrow \nu\bar{\nu} b\bar{b}$ analyses, the selection is similar, except all events with isolated leptons are vetoed and stronger multijet background suppression techniques are applied. As there is a sizable amount of $WH \rightarrow \ell\nu b\bar{b}$ signal that is

* The Tevatron New-Phenomena and Higgs working group can be contacted at TEVNPHWG@fnal.gov. More information can be found at <http://tevnphwg.fnal.gov/>.

TABLE I: The luminosity, mass range explored and reference for the CDF analyses. ℓ stands for e or μ .

	$WH \rightarrow \ell\nu b\bar{b}$ TDT(LDT)	$ZH \rightarrow \nu\bar{\nu} b\bar{b}$ DT(ST)	$ZH \rightarrow \ell^+\ell^- b\bar{b}$ DT(ST)	$H \rightarrow W^+W^- \rightarrow \ell^\pm\nu\ell^\mp\nu$
Luminosity (fb $^{-1}$)	1.7	1.0	1.0	1.9
m_H range (GeV/ c^2)	110-150	110-150	110-150	120-200
Reference	[12]	[13]	[14]	[15]

TABLE II: The luminosity, mass range explored and reference for the DØ $H \rightarrow b\bar{b}$ analyses. ℓ stands for e or μ .

	$WH \rightarrow e\nu b\bar{b}$ DT(ST)	$WH \rightarrow \mu\nu b\bar{b}$ DT(ST)	$WH \rightarrow \not{\ell}\nu b\bar{b}$ DT(ST)	$ZH \rightarrow \nu\bar{\nu} b\bar{b}$ DT(ST)	$ZH \rightarrow \ell^+\ell^- b\bar{b}$
Luminosity (fb $^{-1}$)	1.7	1.7	0.9	0.9	1.1
m_H range (GeV/ c^2)	105-145	105-145	105-135	105-135	105-145
Reference	[16]	[16]	[17]	[17]	[18]

selected by the $ZH \rightarrow \nu\bar{\nu} b\bar{b}$ analyses when the lepton is undetected, the DØ analyses include this as a separate search, referred to as $WH \rightarrow \not{\ell}\nu b\bar{b}$. CDF includes this as part of the acceptance of the $ZH \rightarrow \nu\bar{\nu} b\bar{b}$ search. In the $ZH \rightarrow \nu\bar{\nu} b\bar{b}$ analyses, both CDF and DØ use the dijet invariant mass as the final variable.

The $ZH \rightarrow \ell^+\ell^- b\bar{b}$ analyses require two isolated leptons and two jets, wherein the CDF analysis requires at least one of the jets to be b -tagged while the DØ analysis uses orthogonal sample of events with one and two b -tags. For the DØ analysis a neural network discriminant variables is used as the final variable to set the limits, while CDF uses the output of a 2-dimensional neural network to discriminate between signal and background.

For the $H \rightarrow W^+W^-$ analyses, a large \cancel{E}_T and two opposite-signed, isolated leptons (electrons or muons) are selected, defining three final states (e^+e^- , $e^\pm\mu^\mp$, and $\mu^+\mu^-$). The presence of neutrinos in the final state prevents the direct reconstruction of the Higgs mass, and the final variable used are neural nets (DØ) and likelihoods constructed from matrix element probabilities (CDF). The DØ experiment also contributes three $WH \rightarrow WW^+W^-$ analyses, where the associated W boson and the same-charged W boson from the Higgs decay semi-leptonically, thereby defining six final states containing all decays of the third W boson (of opposite charge). In this case of this analysis, the final variable is a likelihood discriminant formed from several topological variables.

All Higgs signals are simulated using PYTHIA v6.202[3], using CTEQ5L[4] leading order parton distribution functions. The signal cross sections are normalized to next-to-next-to-leading order calculations[5, 6], and branching ratios from HDECAY[7]. For both CDF and DØ, events from multijet (instrumental) backgrounds (“QCD production”) are measured in data, but with different methods. For CDF, inherent backgrounds from other SM processes were generated using PYTHIA, ALPGEN[8], and HERWIG[9] programs. For DØ, inherent backgrounds were generated using PYTHIA, ALPGEN, and COMPHEP[10], with PYTHIA providing parton-showering and hadronization for all the generators. Background processes were normalized using either experimental data or next-to-leading order calculations from MCFM[11].

Values of integrated luminosity, and a reference for more details are given in Table I for CDF analyses and Tables II-III for DØ analyses. The tables also include the value of the Higgs mass for which each set of numbers is derived.

III. COMBINATION PROCEDURES

To gain confidence that the final result does not depend on the details of the statistical formulation, we combine all separate results using both Bayesian and a Frequentist approaches. In both methods, histograms summarizing the distributions of the final variables reconstructed for each event are used, rather than as single integrated values. Systematic uncertainties enter as uncertainties on the expected number of signal and background events in each

TABLE III: The luminosity, mass range explored, and reference for the $D\bar{O} WH \rightarrow WW^+W^-$ and $H \rightarrow W^+W^-$ analyses.

	$WW^+W^- \rightarrow e^\pm \nu e^\pm \nu$	$H \rightarrow W^+W^- \rightarrow e^\pm \nu e^\mp \nu$	$H \rightarrow W^+W^- \rightarrow e^\pm \nu \mu^\mp \nu$
	$WW^+W^- \rightarrow e^\pm \nu \mu^\pm \nu$	$H \rightarrow W^+W^- \rightarrow e^\pm \nu \mu^\mp \nu$	
	$WW^+W^- \rightarrow \mu^\pm \nu \mu^\pm \nu$	$H \rightarrow W^+W^- \rightarrow \mu^\pm \nu \mu^\mp \nu$	
Luminosity (fb $^{-1}$)	1.1	1.0	0.6
m_H range (GeV/ c^2)	120-200	120-200	120-200
Reference	[19]	[20, 21]	[22]

analysis, as well as on the shapes of the histograms. Both methods use likelihood calculations based upon Poisson probabilities.

A. Frequentist Method

The Frequentist technique relies on the CL_s method, using a log-likelihood ratio (LLR) as test statistic[1], as given by:

$$LLR_n = 2 \sum_{i=1}^N (s_i - n_i \text{Log}(1 + s_i/b_i)) \quad (1)$$

where n denotes the hypothesis being tested (*e.g.*, background-only or observed data) and the sum runs over the number of bins (and/or analyses) being combined. The value of CL_s is then defined as the normalization of the signal+background hypothesis (CL_{s+b}) by the background-only hypothesis (CL_b). This construction reduces the ambiguity of “unphysical” results (*e.g.*, negative cross section limits) and separates properties of the estimator from that of the quantity being probed.

B. Bayesian Method

Because there is no information on the production cross section for the Higgs, the Bayesian technique[2] assigns a flat prior for the total number of selected Higgs events. For a given Higgs mass, the combined likelihood is a product of the likelihoods in the individual channels, each of which is a product over histogram bins:

$$\mathcal{L}(R, \vec{s}, \vec{b} | \vec{n}, \vec{\theta}) = \prod_{i=1}^{N_C} \prod_{j=1}^{Nbins} \mu_{ij}^{n_{ij}} e^{-\mu_{ij}} / n_{ij}! \times \prod_{k=1}^{n_{np}} e^{-\theta_k^2/2} \quad (2)$$

where the first product is over the number of channels (N_C), and the second product is over histogram bins containing n_{ij} observed events. These histograms are binned in the final variables chosen by the individual analyses, such as m_{jj} , neural network outputs in 1D and 2D, or matrix-element likelihoods. The parameters that contribute to the expected bin contents are $\mu_{ij} = R \times s_{ij}(\vec{\theta}) + b_{ij}(\vec{\theta})$ for the channel i and the histogram bin j . The likelihood function also contains truncated Gaussian constraints on the nuisance parameters θ_k , which define the sensitivity of the predicted signal and background estimates to systematic uncertainties, which can take the form of uncertainties on overall rates, as well as the shapes of the histograms used for combination. These systematic uncertainties can be several times larger than the expected SM signal, and are therefore important in the limit calculation. The truncation is applied so that no prediction of any signal or background in any bin is negative. The posterior density function is then integrated over all parameters (including correlations) except for R , and a 95% credibility level upper limit on R is estimated by calculating the value of R that corresponds to 95% of the area of the resulting distribution.

TABLE IV: Systematic uncertainties on the signal contributions for CDF's $WH \rightarrow \ell\nu b\bar{b}$ loose double tag (LDT) channel. Systematic uncertainties are listed by name. No shape uncertainties are provided, nor are the MC statistics included in the template histogram bins for this channel. Uncertainties are relative, fractional errors and are symmetric unless otherwise indicated.

Contribution	W+HF	Mistags	Top	Diboson	Non-W	Signal
LUMI	0	0	0	0	0	0.04
CDFLUMI	0	0	0	0	0	0.05
CDFBTAGSF	0	0	0	0	0	0.08
CDFLEPTONID	0	0	0	0	0	0.02
CDFJES	0	0	0	0	0	0.03
CDFHF	0.33	0	0	0	0	0
CDFMISTAG	0	0.22	0	0	0	0
TTXSEC	0	0	0.135	0	0	0
DIBOSON	0	0	0	0.16	0	0
CDFQCD	0	0	0	0	0.17	0
NNLO	0	0	0	0	0	0.01
ISRFSRPDF	0	0	0	0	0	0.04

C. Systematic Uncertainties

Systematic uncertainties differ between experiments and analyses, and they affect the rates and shapes of the predicted signal and background histograms in correlated ways. The combined results incorporate the provided sensitivity of the predictions to the unknown values of the nuisance parameters, and correlations are included, between rates and shapes, between signals and backgrounds, and between channels within experiments and between experiments. Detailed discussions of these issues can be found in the individual analysis notes[1, 2]. Here we will consider only the largest contributions and correlations among and within the two experiments.

1. Correlated Systematics

The uncertainty on the production rates for top-quark processes ($t\bar{t}$ and single-top) and electroweak processes (WW , WZ , and ZZ) are taken as correlated between the two experiments. As the methods of measuring the multijet (QCD) backgrounds differ between CDF and DØ, there is no correlation assumed for this uncertainty.

2. CDF Systematics

The dominant systematic uncertainties for the CDF analyses are shown in Tables IV through X. For $H \rightarrow b\bar{b}$, the largest uncertainties on signal arise from the b -tagging scale factor (5.3-16%), jet energy scale (1-20%), and MC modeling (2-10%). For $H \rightarrow W^+W^-$, the largest contributing uncertainty comes from MC modeling (5%). For inherent backgrounds, the uncertainties on the expected rates range from 11-40% (depending on background). Because the largest background contributions are measured using data, these uncertainties are treated as uncorrelated for the $H \rightarrow b\bar{b}$ channels. For the $H \rightarrow W^+W^-$ channel, the luminosity uncertainty is taken to be correlated between signal and background. The differences between treating the remaining uncertainties to be correlated or uncorrelated is less than 5%.

3. DØ Systematics

The dominant systematic uncertainties for DØ analyses are shown in Table XI. The $H \rightarrow b\bar{b}$ analyses have an uncertainty on the b -tagging rate of 3-10% per tagged jet. These analyses also have an uncertainty on the jet

TABLE V: Systematic uncertainties for the CDF’s $WH \rightarrow \ell\nu b\bar{b}$ tight double-tag (TDT) channel. Systematic uncertainties are listed by name. No shape uncertainties are provided, nor are the MC statistics included in the template histogram bins for this channel. Uncertainties are relative, fractional errors and are symmetric unless otherwise indicated.

Contribution	W+HF	Mistags	Top	Diboson	Non-W	Signal
LUMI	0	0	0	0	0	0.04
CDFLUMI	0	0	0	0	0	0.05
CDFBTAGSF	0	0	0	0	0	0.16
CDFLEPTONID	0	0	0	0	0	0.02
CDFJES	0	0	0	0	0	0.03
CDFHF	0.34	0	0	0	0	0
CDFMISTAG	0	0.15	0	0	0	0
TTXSEC	0	0	0.20	0	0	0
DIBOSON	0	0	0	0.25	0	0
CDFQCD	0	0	0	0	0.20	0
NNLO	0	0	0	0	0	0.01
ISRFSRPDF	0	0	0	0	0	0.1

measurement and acceptance of 6-9% (jet identification or jet ID, energy scale, and jet smearing). For the $H \rightarrow W^+W^-$ and $WH \rightarrow WW^+W^-$, the largest uncertainties are associated with lepton measurement and acceptance. These values range from 2-11% depending on the final state. The largest contributing factor to all analyses is the uncertainty on the cross sections for inherent background at 6-18%. These systematics are assumed to apply to both signal and background processes. All systematic uncertainties arising from the same source are taken to be correlated between signal and background, as detailed in Table XI.

IV. COMBINED RESULTS

Using the combination procedures outlined above, we extract limits on SM Higgs boson production $\sigma \times BR^*(H \rightarrow X)$ in $p\bar{p}$ collisions at $\sqrt{s} = 1.96$ TeV.

To facilitate model transparency and to accommodate analyses with different degrees of sensitivity, we present our results in terms of the ratio of limits set to the SM cross sections as a function of Higgs mass. A value of < 1 would indicate a Higgs mass excluded at 95% CL. The expected and observed 95% upper limit ratios to the SM cross section for the combined CDF and $D\bar{O}$ analyses are shown in Figure 1. The observed and median expected limit ratios are listed for selected Higgs masses in Table XII, with observed(expected) values of 7.8(4.3) at $m_H = 115$ GeV/ c^2 and 1.4(2.5) at $m_H = 160$ GeV/ c^2 .

These results represent an improvement in search sensitivity over those obtained for individual experiments, which have set observed(expected) limit ratios of 8.3(6.0) for $D\bar{O}$ and 8.6(6.4) for CDF at $m_H = 115$ GeV/ c^2 and of 3.5(4.6) for $D\bar{O}$ and 2.0(3.1) for CDF at $m_H = 160$ GeV/ c^2 .

TABLE VI: Systematic uncertainties for CDF’s $ZH \rightarrow \nu\bar{\nu}b\bar{b}$ single-tag (ST) channel. Systematic uncertainties are listed by name. Systematic uncertainties with shapes provided are indicated with an “s”. Systematic uncertainties in which limited Poisson statistical errors in the Monte Carlo are provided are indicated with a “p”. Uncertainties are relative, fractional errors and are symmetric unless otherwise indicated.

Contribution	Mistag	QCD ₁ p	Single $t(s)$ p	Single $t(t)$ p	$t\bar{t}$ p	WW p
CDFLUMI	0	0	0.06	0.06	0.06	0.06
CDFBTAGSF	0	0.04	0.04	0.04	0.04	0.04
CDFJES	0	$+0.23^s$ -0.16^s	0.08s	$+0.08^s$ -0.12^s	-0.03^s $+0.04^s$	$+0.16^s$ -0.08^s
CDFTRIGEFF	0.01	0.03	0.03	0.03	0.03	0.03
PDF	0	0	0.02	0.02	0.02	0.02
CDFQCDNORM	0	0.03	0	0	0	0
ZXSEC	0	0	0	0	0	0
WXSEC	0	0	0	0	0	0
VVXSEC	0	0	0	0	0	0.12
TTXSEC	0	0	0	0	0.11	0
TXSEC	0	0	0.13	0.13	0	0
CDFFAKELEPTONVETO	0.02	0.02	0	0	0	0
CDFLEPTONIDVETO	0	0	0.02	0.02	0.02	0.02
ISR	0	0	0	0	0	0
FSR	0	0	0	0	0	0
CDFMISTAG	0.21s	0	0	0	0	0

Contribution	WZ p	ZZ p	$W \rightarrow e\nu$ p	$W \rightarrow \mu\nu$ p	$W \rightarrow \tau\nu$ p
CDFLUMI	0.06	0.06	0.06	0.06	0.06
CDFBTAGSF	0.043	0.043	0.043	0.043	0.043
CDFJES	$+0.16^s$ -0.14^s	$+0.09^s$ -0.14^s	0.22^s -0.18^s	0.17^s -0.14^s	0.29^s -0.07^s
CDFTRIGEFF	0.03	0.03	0.03	0.03	0.03
PDF	0.02	0.02	0.02	0.02	0.02
CDFQCDNORM	0	0	0	0	0
ZXSEC	0	0	0	0	0
WXSEC	0	0	0.40	0.40	0.4
VVXSEC	0.115	0.115	0	0	0
TTXSEC	0	0	0	0	0
TXSEC	0	0	0	0	0
CDFFAKELEPTONVETO	0	0	0	0	0
CDFLEPTONIDVETO	0.02	0.02	0.02	0.02	0.02
ISR	0	0	0	0	0
FSR	0	0	0	0	0
CDFMISTAG	0.21	0	0	0	0

Contribution	$Z \rightarrow ee$ p	$Z \rightarrow \mu\mu$ p	$Z \rightarrow \tau\tau$ p	$Z \rightarrow \nu\nu$	ZH 120 GeV p	WH 120 GeV p
CDFLUMI	0.06	0.06	0.06	0.06	0.06	0.06
CDFBTAGSF	0.043	0.043	0.043	0.043	0.043	0.043
CDFJES	$+1.0^s$ -0^s	$+0.06^s$ -0.18^s	$+0.25^s$ -0.5^s	$+0.15^s$ -0.10^s	$+0.07^s$ -0.07^s	$+0.07^s$ -0.06^s
CDFTRIGEFF	0.03	0.03	0.03	0.03	0.03	0.03
PDF	0.02	0.02	0.02	0.02	0.02	0.02
CDFQCDNORM	0	0	0	0	0	0
ZXSEC	0.40	0.40	0.40	0.40	0	0
WXSEC	0	0	0	0	0	0
VVXSEC	0	0	0	0	0	0
TTXSEC	0	0	0	0	0	0
TXSEC	0	0	0	0	0	0
CDFFAKELEPTONVETO	0	0	0	0	0.02	0.02
CDFLEPTONIDVETO	0.02	0.02	0.02	0.02	0	0
ISR	0	0	0	0	$+0.018$ -0.024	$+0.035$ -0.003
FSR	0	0	0	0	$+0.001$ -0.006	$+0.023$ -0.013
CDFMISTAG	0	0	0	0	0	0

TABLE VII: Systematic uncertainties for CDF’s $ZH \rightarrow \nu\bar{\nu}b\bar{b}$ double-tag (DT) channel. Systematic uncertainties are listed by name. Systematic uncertainties with shapes provided are indicated with an “s”. Systematic uncertainties in which limited Poisson statistical errors in the Monte Carlo are provided are indicated with a “p”. Uncertainties are relative, fractional errors and are symmetric unless otherwise indicated.

Contribution	Mistag	QCD ₁ p	Single $t(s)$ p	Single $t(t)$ p	$t\bar{t}$ p	WW p
CDFLUMI	0	0	0.06	0.06	0.06	0.06
CDFBTAGSF	0	0.09	0.09	0.09	0.09	0.09
CDFJES	0	$^{+0}_{-0.10}$ s	$^{+0.04}_{-0.07}$	$^{+0.2}_{-0}$ s	$^{-0.002}_{+0.02}$ s	0 s
CDFTRIGEFF	0.02	0.03	0.03	0.03	0.03	0.03
PDF	0	0	0.02	0.02	0.02	0.02
CDFQCDNORM	0	0.05	0	0	0	0
ZXSEC	0	0	0	0	0	0
WXSEC	0	0	0	0	0	0
VVXSEC	0	0	0	0	0	0.12
TTXSEC	0	0	0	0	0.11	0
TXSEC	0	0	0.13	0.13	0	0
CDFFAKELEPTONVETO	0.02	0.02	0	0	0	0
CDFLEPTONIDVETO	0	0	0.02	0.02	0.02	0.02
ISR	0	0	0	0	0	0
FSR	0	0	0	0	0	0
CDFMISTAG2	$^{+0.90}_{-0.71}$ s	0	0	0	0	0

Contribution	WZ p	ZZ p	$W \rightarrow e\nu$ p	$W \rightarrow \mu\nu$ p	$W \rightarrow \tau\nu$ p
CDFLUMI	0.06	0.06	0.06	0.06	0.06
CDFBTAGSF	0.09	0.09	0.09	0.09	0.09
CDFJES	$^{+0.17}_{-0.09}$ s	$^{+0.08}_{-0.20}$ s	$^{0.67}_{-0}$ s	$^{0.14}_{-0.21}$ s	$^{0.2}_{+0.1}$ s
CDFTRIGEFF	0.03	0.03	0.03	0.03	0.03
PDF	0.02	0.02	0.02	0.02	0.02
CDFQCDNORM	0	0	0	0	0
ZXSEC	0	0	0	0	0
WXSEC	0	0	0.40	0.40	0.4
VVXSEC	0.115	0.115	0	0	0
TTXSEC	0	0	0	0	0
TXSEC	0	0	0	0	0
CDFFAKELEPTONVETO	0	0	0	0	0
CDFLEPTONIDVETO	0.02	0.02	0.02	0.02	0.02
ISR	0	0	0	0	0
FSR	0	0	0	0	0
CDFMISTAG	0.21	0	0	0	0

Contribution	$Z \rightarrow ee$	$Z \rightarrow \mu\mu$	$Z \rightarrow \nu\nu$	ZH 120 GeV p	WH 120 GeV p
CDFLUMI	–	–	0.06	0.06	0.06
CDFBTAGSF	–	–	0.09	0.09	0.09
CDFJES	–	–	$^{+0.17}_{-0.13}$ s	$^{+0.05}_{-0.06}$ s	$^{+0.04}_{-0.07}$ s
CDFTRIGEFF	–	–	0.03	0.03	0.03
PDF	–	–	0.02	0.02	0.02
CDFQCDNORM	–	–	0	0	0
ZXSEC	–	–	0.40	0	0
WXSEC	–	–	0	0	0
VVXSEC	–	–	0	0	0
TTXSEC	–	–	0	0	0
TXSEC	–	–	0	0	0
CDFFAKELEPTONVETO	–	–	0	0.02	0.02
CDFLEPTONIDVETO	–	–	0.02	0	0
ISR	–	–	0	$^{+0.049}_{-0.026}$	$^{+0.018}_{+0.024}$
FSR	–	–	0	$^{-0.006}_{+0.015}$	$^{+0.042}_{+0.004}$
CDFMISTAG	–	–	0	0	0

TABLE XI: List of leading correlated systematic uncertainties for the $D\bar{O}$ analyses. The values for the systematic uncertainties are the same for the $ZH \rightarrow \nu\bar{\nu}b\bar{b}$ and $WH \rightarrow \ell\nu b\bar{b}$ channels. All uncertainties with a common origin are considered 100% correlated across channels. The correlated systematic uncertainty on the background cross section (σ) is itself subdivided according to the different background processes in each analysis.

Source	$WH \rightarrow e\nu b\bar{b}$ DT(ST)	$WH \rightarrow \mu\nu b\bar{b}$ DT(ST)	$H \rightarrow W^+W^-, WH \rightarrow WW^+W^-$
Luminosity (%)	6.1	6.1	6.1
Jet Energy Scale (%)	3.0	3.0	3.0,0
Jet ID (%)	3.0	3.0	0
Electron ID/Trigger (%)	6.0	0	2.3-10,11.0
Muon ID/Trigger (%)	0	11	7.7-10,11.0
b -Jet Tagging (%)	9.2(4.6)	9.2(4.6)	0
Background σ (%)	6.0-18.0	6.0-18.0	6.0-18.0

Source	$ZH \rightarrow \nu\bar{\nu}b\bar{b}$ DT(ST)	$ZH \rightarrow e^+e^-b\bar{b}$	$ZH \rightarrow \mu^+\mu^-b\bar{b}$
Luminosity (%)	6.1	6.1	6.1
Jet Energy Scale (%)	5.0	2.0	2.0
Jet ID (%)	7.1	5.0	5.0
Electron ID (%)	0	4.0	0
Muon ID (%)	0	0	4.0
b -Jet Tagging (%)	9.6	7.5(3.0)	7.5(3.0)
Background σ (%)	6.0-18.0	6.0-18.0	6.0-18.0

TABLE XII: Median expected and observed 95% CL cross section ratios for the combined CDF and DØ analyses.

	110 GeV/c ²	115 GeV/c ²	120 GeV/c ²	140 GeV/c ²	160 GeV/c ²	180 GeV/c ²	200 GeV/c ²
Expected	3.5	4.3	4.8	4.2	2.5	3.4	7.5
Observed	7.0	7.8	10.4	3.5	1.4	2.3	6.2

- [1] DØ Collaboration, “Limits on Standard Model Higgs Boson Production”, DØ Conference Note 5487,
- [2] CDF Collaboration, “Combined Upper Limit on Standard Model Higgs Boson Production” CDF/ANAL/EXOTIC/PUBLIC/8941
- [3] T. Sjostrand, L. Lonnblad and S. Mrenna, “PYTHIA 6.2: Physics and manual,” [arXiv:hep-ph/0108264]
- [4] H. L. Lai *et al.*, *Improved Parton Distributions from Global Analysis of Recent Deep Inelastic Scattering and Inclusive Jet Data*, Phys. Rev D **55** (1997) 1280
- [5] S. Catani, D. de Florian, M. Grazzini and P. Nason, “Soft-gluon resummation for Higgs boson production at hadron colliders,” JHEP **0307**, 028 (2003), [arXiv:hep-ph/0306211]
- [6] K. A. Assamagan *et al.* [Higgs Working Group Collaboration], “The Higgs working group: Summary report 2003,” [arXiv:hep-ph/0406152]
- [7] A. Djouadi, J. Kalinowski and M. Spira, “HDECAY: A program for Higgs boson decays in the standard model and its supersymmetric extension,” Comput. Phys. Commun. **108**, 56 (1998) [arXiv:hep-ph/9704448]
- [8] M. L. Mangano, M. Moretti, F. Piccinini, R. Pittau and A. D. Polosa, “ALPGEN, a generator for hard multiparton processes in hadronic collisions,” JHEP **0307**, 001 (2003) [arXiv:hep-ph/0206293]
- [9] G. Corcella *et al.*, “HERWIG 6: An event generator for hadron emission reactions with interfering gluons (including supersymmetric processes),” JHEP **0101**, 010 (2001) [arXiv:hep-ph/0011363]
- [10] A. Pukhov *et al.*, “CompHEP: A package for evaluation of Feynman diagrams and integration over multi-particle phase space. User’s manual for version 33,” [arXiv:hep-ph/9908288]
- [11] J. Campbell and R. K. Ellis, “Next-to-leading order corrections to W + 2jet and Z + 2jet production at hadron colliders,” Phys. Rev. D **65**, 113007 (2002), [arXiv:hep-ph/0202176]
- [12] CDF Collaboration, “Search for Higgs Boson Production in Association with W Boson with 1.7 fb⁻¹,” CDF/ANAL/EXOTIC/PUBLIC/8957
- [13] CDF Collaboration, “Search for the Standard Model Higgs Boson in the Missing Et and B-jets Signature” CDF/ANAL/EXOTIC/PUBLIC/8442.
- This combination uses an updated version of the analysis described in CDF Note 8362.
- [14] CDF Collaboration, “Search for ZH in 1 fb⁻¹,” CDF/PUB/EXOTIC/PUBLIC/8742.
- [15] CDF Collaboration, “Search for H_tWW Production Using 1.9 fb⁻¹,” CDF/ANAL/EXOTIC/CDFR/8923.
- [16] DØ Collaboration, “Search for WH Production at $\sqrt{s} = 1.96$ TeV with Neural Networks,” DØ Conference Note 5472
- [17] DØ Collaboration, “A Search for the Standard Model Higgs boson using the $ZH \rightarrow \nu\bar{\nu}b\bar{b}$ channel in $p\bar{p}$ Collisions at $\sqrt{s} = 1.96$ TeV”, DØ Conference Note 5353
- [18] DØ Collaboration, “A Search for $ZH \rightarrow \ell^+\ell^-\bar{b}\bar{b}$ Production at DØ in $p\bar{p}$ Collisions at $\sqrt{s} = 1.96$ TeV,” DØ Conference Note 5482
- [19] DØ Collaboration, “Search for associated Higgs boson production $WH \rightarrow WWW^* \rightarrow \ell^\pm\nu\ell'^\pm\nu' + X$ in $p\bar{p}$ collisions at $\sqrt{s} = 1.96$ TeV,” DØ Conference Note 5485
- [20] DØ Collaboration, “Search for the Higgs boson in $H \rightarrow WW^* \rightarrow l^+l^- (ee, e\mu)$ decays with 950 pb⁻¹ at DØ in Run II,” DØ Conference Note 5063
- [21] DØ Collaboration, “Search for the Higgs boson in $H \rightarrow WW^* \rightarrow \mu\mu$ decays with 930 pb⁻¹ at DØ in Run II,” DØ Conference Note 5194
- [22] DØ Collaboration, “Search for the Higgs boson in $H \rightarrow WW^* \rightarrow e\mu$ decays with 0.6 fb⁻¹ at DØ in Run IIb,” DØ Conference Note 5489

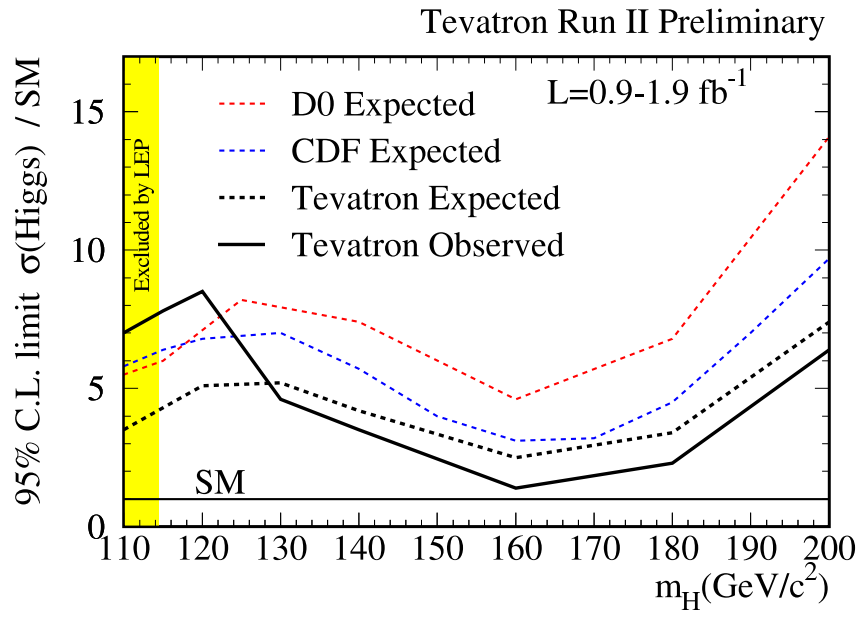


FIG. 1: Expected and observed 95% CL cross section ratios for the combined CDF and DØ analyses. Also shown are the expected 95% CL ratios for the CDF and DØ experiments alone.